Original Article

Three-dimensional imaging analysis for the diagnosis of dural ossification in thoracic ossification of the ligamentum flavum: a multicenter study

Chen Yan[1#], Shi-Yong Ling[2#], Tian-Yi Zhao[1#], Ying Tan[3], Tao Liu[3], Jun Shen[4], Guo-Dong Shi[1], Jing-Chuan Sun[1], Jian-Gang Shi[1]

[1]Department of Orthopedic Surgery, Spine Center, Changzheng Hospital, Second Military Medical University, Shanghai, China; [2]Department of Orthopedic Surgery, Zhabei Central Hospital, Shanghai, China; [3]Department of Spinal Surgery, Weifang Traditional Chinese Medicine Hospital, Weifang, China; [4]Department of Spinal Surgery, Suzhou Municipal Hospital, Nanjing Medical University, Suzhou, China

Contributions: (I) Conception and design: C Yan, JC Sun, JG Shi; (II) Administrative support: JG Shi, J Shen, T Liu; (III) Provision of study materials or patients: GD Shi, SY Ling; (IV) Collection and assembly of data: SY Ling, TY Zhao, Y Tan; (V) Data analysis and interpretation: C Yan, JC Sun; (VI) Manuscript writing: All authors; (VII) Final approval of manuscript: All authors.

[#]These authors contributed equally to this work.

Correspondence to: Jing-Chuan Sun, MD; Jian-Gang Shi, MD. Department of Orthopedic Surgery, Spine Center, Changzheng Hospital, Second Military Medical University, No. 415 Fengyang Road, Shanghai 200003, China. Email: sumhm11@yeah.net; shijiangang3@163.com.

Background: Unforeseen dural ossification (DO) increases the risk of complications in the surgical management of thoracic ossification of the ligamentum flavum (OLF). Several methods have been proposed to identify DO; however, these approaches either have low diagnostic accuracy or poor feasibility. Therefore, we aimed to determine the relationship between DO and the severity and range of thoracic OLF compression using a 3-dimensional (3D) imaging analysis and to evaluate its superiority in diagnosing DO over conventional measurement methods.

Methods: A total of 114 consecutive patients who underwent decompressive laminectomy for thoracic OLF in 4 institutions were retrospectively enrolled and divided into DO and non-DO groups. Univariate analysis was performed to determine the relationship between OLF compression and DO. We measured the 3D occupying ratio (OR; 3D OR = OLF volume/normal canal volume × 100%), calculated its cutoff values, and compared its diagnostic value in DO with that of conventional 1D and 2D radiological parameters in the whole thoracic spine.

Results: The 3D OR in the DO group (50.9%±7.9%) was significantly higher than that in the non-DO group (30.8%±7.5%; P<0.01). The overall reliability and reproducibility for measurements of the 3D OR (intra- and interobserver correlation coefficients 0.94 and 0.90, respectively) were excellent. Thus, the 3D OR could be used as an indicator to distinguish between DO and non-DO, with high diagnostic accuracy (91.2%). Moreover, a 3D OR of >43%, known as the "ossification zone", was indicative of DO in OLF, whereas a value of <37% was considered the "safe zone". Additionally, the 3D OR [area under the curve (AUC) =0.98, 95% confidence interval (CI): 0.93–0.99] showed a statistically higher diagnostic value for DO in the upper, middle, lower, and whole thoracic spine than did both 1D (AUC =0.81; 95% CI: 0.73–0.88) and 2D (AUC =0.87; 95% CI: 0.79–0.92) parameters (P<0.01).

Conclusions: DO was significantly associated with the severity and range of OLF compression. The 3D OR could be used as a critical diagnostic indicator for identifying DO in the whole thoracic spine, owing to its superiority over conventional radiological parameters. Classification of the 3D OR could maximize the clinical feasibility and thus help surgeons to decrease the incidence of DO-related surgical complications.

Keywords: Thoracic ossification of the ligamentum flavum; three-dimensional imaging analysis; dural ossification (DO); diagnosis; conventional measurement

Submitted Apr 26, 2022. Accepted for publication Oct 30, 2022. Published online Nov 14, 2022.
doi: 10.21037/qims-22-418
View this article at: https://dx.doi.org/10.21037/qims-22-418

Introduction

Ossification of the ligamentum flavum (OLF) presents as a pathological replacement of the ligamentum flavum with hypertrophic lamina bone and has been recognized as the main cause of thoracic spinal stenosis and myelopathy (1-4). Due to the progression of OLF and its poor response to conservative therapy, surgical decompression is generally considered to be the best treatment option (5). Potential sequelae of chronic OLF are the compression and subsequent ossification of the dura mater, resulting in an inseparable osseous fusion between the ligamentum flavum and the dura mater (1,6,7). For surgeons, unforeseen dural ossification (DO) may increase the risk of intraoperative complications, such as cerebrospinal fluid (CSF) leakage and spinal cord injury (3,7-9). Preoperative diagnosis of DO assists surgeons in making comprehensive preparations for the surgical procedure. Although the incidence of DO in patients with OLF is as high as 43.4%, the accurate diagnosis of DO has presented a difficult problem for surgical management (8,10). Radiological studies regarding OLF-DO are relatively rare, and the diagnostic accuracy of imaging signs still needs to be improved (11,12). Furthermore, there are variations in how the slices through tissues are obtained based on the spinal curvature, especially for the upper or middle thoracic spine, which might lead to deviations in the results of conventional measurement methods (13-16). Therefore, most of the current findings can only be applied to the lower thoracic spine, despite nearly 50% of DOs being located in the upper and middle segments (9,12,14,15).

Combining previous studies and clinical observations, we find that DO frequently occurs in the segment with the most severe compression on sagittal computed tomography (CT) images (17,18). Moreover, axial images illustrate that DO is often observed on multiple slices and not just on a single slice (6,8,19,20). Therefore, we speculate that the formation of DO is associated with the severity of OLF compression of the dura mater and the contact area of the OLF and the dura mater. Considering that OLF compression is not a 2-dimensional (2D) problem and is rather a 3D problem (14,21,22), a novel 3D imaging analysis based on CT scans was used in the present study. This may correct the measurement deviation caused by spinal curvature with multiplanar reconstruction (MPR). We sought to test this hypothesis by using the 3D imaging analysis and evaluate its superiority in diagnosing DO in the whole thoracic spine over the conventional measurement methods. We present the following article in accordance with the STARD reporting checklist (available at https://qims.amegroups.com/article/view/10.21037/qims-22-418/rc).

Methods

Patients

This retrospective study analyzed 397 consecutive patients who underwent laminectomy for thoracic OLF in four institutions (Shanghai Changzheng Hospital, Shanghai Zhabei Central Hospital, Weifang Traditional Chinese Medicine Hospital, and Suzhou Municipal Hospital) between May 2014 and April 2019. Thoracic OLF diagnosis was based on the patient's medical history, clinical symptoms, and radiological information. Neurological deterioration was considered the indication for surgical treatment. The exclusion criteria were as follows: (I) a history of spinal trauma, tumor, deformity, or surgery; (II) accompanying thoracic ventral compressive lesions; (III) diffuse idiopathic skeletal hyperostosis; and (IV) incomplete or ambiguous data.

Intraoperative evidence of DO included the following: (I) obvious fusion of the ossified dura and OLF; (II) the occurrence of dural tears and CSF leakage during resection due to adhesion of the ossified dura and OLF; and (III) OLF and ossified dura found in the resected ossified mass. According to intraoperative evidence of DO, these patients were divided into non-DO and DO groups (*Figure 1*). The patients' clinical characteristics were recorded, including sex, age, body mass index (BMI), diabetes mellitus (DM), hypertension (HTN), the number of ossified segments, and the segment of maximum compression. This study was conducted in accordance with the Declaration of Helsinki (as

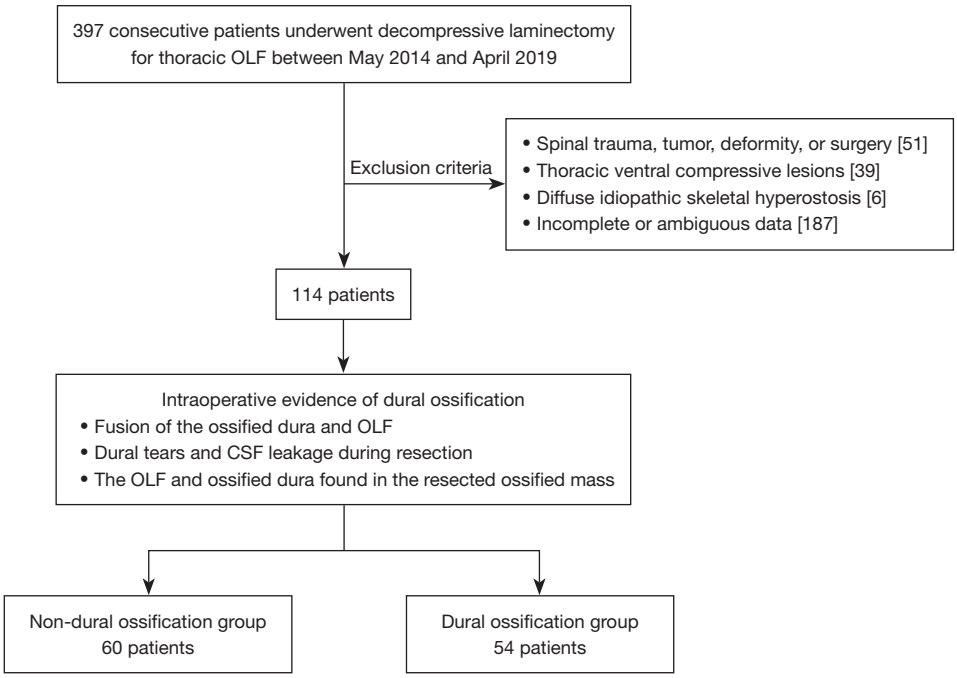

Figure 1 Patient screening and classification flowchart. OLF, ossification of the ligamentum flavum; CSF, cerebrospinal fluid.

revised in 2013) and was approved by and registered with the institutional review board of Shanghai Changzheng Hospital. The requirement for individual informed consent for this retrospective analysis was waived.

Radiological measurements

Preoperative CT images of the thoracic spine obtained using a Philips Brilliance 256-slice CT (Philips Healthcare, Amsterdam, The Netherlands) or Siemens 64-detector CT (Siemens Healthcare. Erlangen, Germany) were available for all 114 patients. The following imaging parameters were used for CT scanning: 120 kVp/50 mAs, slice thickness 1 mm, slice interval 1 mm, matrix 512×512 pixels, collimation 128×0.625 mm, duration 0.5 s, and standard resolution algorithms with iDose4 iterative reconstruction. All CT images were assessed by 3 independent and well-experienced observers with more than 6 years of experience in the practice of spinal surgery who were blinded to the grouping and medical information of all included patients. Each observer measured all radiological parameters 3 times and recorded the mean values of the 3 measurements.

To investigate the relationship between DO and the severity and range of OLF compression of the dura mater, a 3D occupying ratio (OR) was used based on multidimensional imaging analysis software, which could assess OLF compression from the coronal, axial, and sagittal views. Preoperative CT images with Digital Imaging and Communication in Medicine (DICOM) data were imported into Mimics software 19.0 (Materialise, Inc., Leuven, Belgium) for measurement of the 3D OR.

To evaluate the 3D imaging analysis and conventional measurement methods in the diagnosis of DO, the 1D OR and 2D OR, as the most accurate diagnostic indicators of OLF-DO in previous studies, were compared with the 3D OR (12,15). The diagnostic values of DO among the 1D, 2D, and 3D ORs were compared in the upper, middle, lower, and whole thoracic spine. As the conventional measurement methods, the 1D and 2D ORs were measured using IMPAX 6.0 software (AGFA, Inc., Mortsel, Belgium). The detailed measurement methods are described in the following sections.

1D OR

The OLF thickness was defined as the maximum thickness of the unilateral ossified mass (*Figure 2A*). The spinal canal distance was defined as the distance from the lamina to the midpoint of the posterior vertebral wall (*Figure 2B*). The bilateral ORs were measured, and the larger value was considered the 1D OR. The 1D OR was calculated using

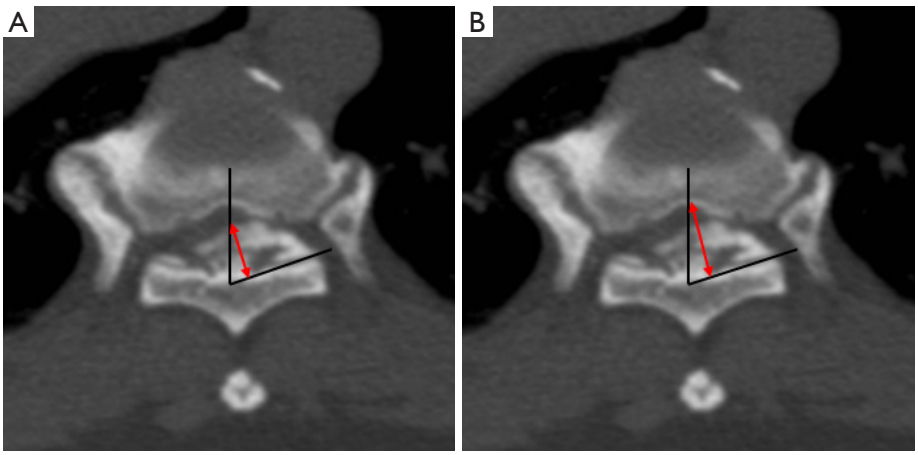

Figure 2 Measurement of the 1D OR. The 1D OR was calculated as follows: OLF thickness/spinal canal distance × 100%. (A) In the axial view, the OLF thickness was defined as the maximum thickness of the unilateral ossified mass (red arrow). (B) In the axial view, the spinal canal distance was defined as the distance (red arrow) from the lamina to the midpoint of the posterior vertebral wall (black line). 1D, 1-dimensional; OR, occupying ratio; OLF, ossification of the ligamentum flavum.

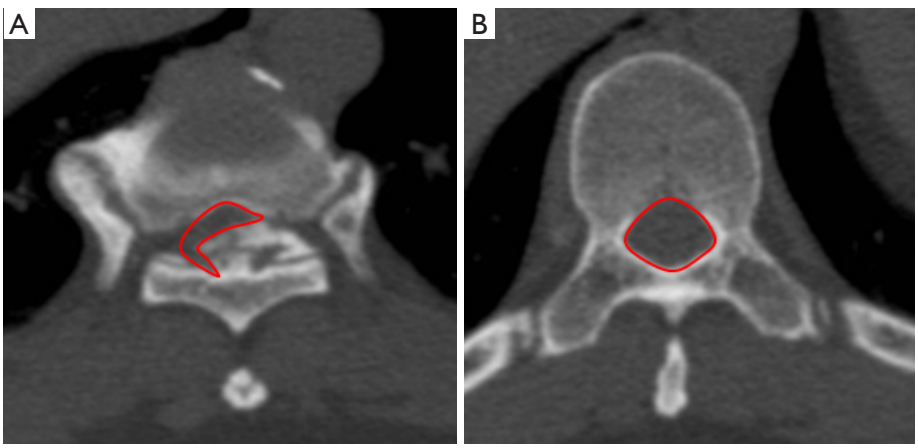

Figure 3 Measurement of the 2D OR. The 2D OR was calculated as follows: (1 – available canal area/normal canal area) × 100%. (A) In the axial view, the available canal area was defined as the available cross-sectional area of the narrowest spinal canal (red polygon). (B) In the axial view, the normal canal area was defined as the cross-sectional area of the spinal canal with the widest distance between the pedicles and no ossification in the same segment (red polygon). 2D, 2-dimensional; OR, occupying ratio.

the following formula: 1D OR = OLF thickness/spinal canal distance × 100%.

2D OR

The available canal area was defined as the available cross-sectional area of the narrowest spinal canal (*Figure 3A*). The normal canal area was measured as the cross-sectional area of the spinal canal with the widest distance between the pedicles and no ossification at the same segment (*Figure 3B*). The 2D OR was calculated using the following formula: 2D OR = (1 – available canal area/normal canal area) × 100%.

3D OR

The procedures of 3D measurement using Mimics software comprised the following 5 steps. (I) The initial outline of the normal spinal canal was identified using the Multiple slice editor and Interpolation button. (II) In the pedicle region, the outline of the normal spinal canal could be determined directly. In the region without pedicles, the cross-sectional contour of the spinal canal with the widest

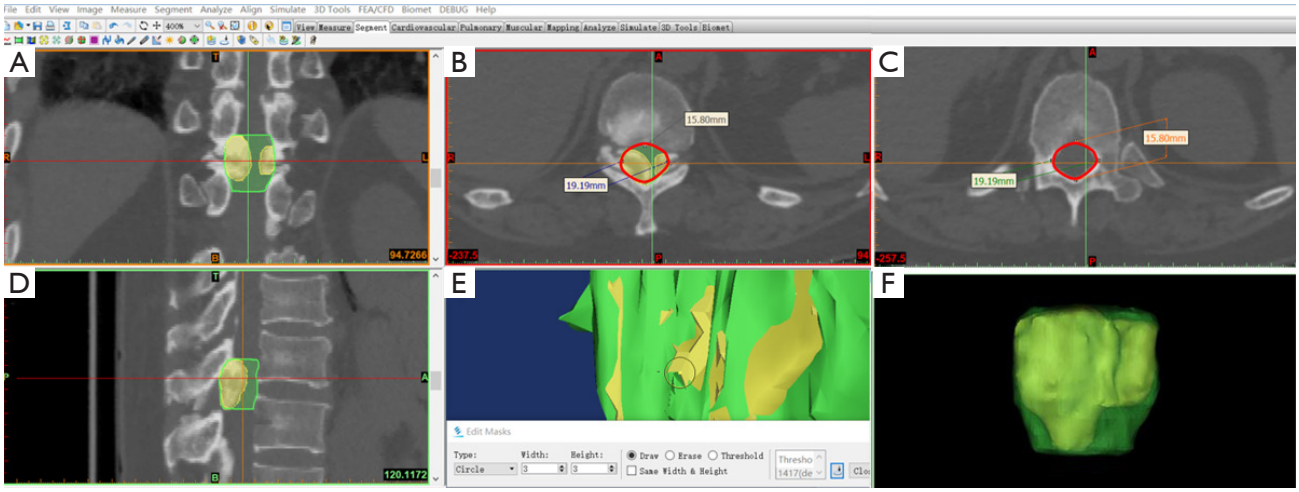

Figure 4 Measurement of the 3D OR using the Mimics software. The outlines of the OLF mass (yellow) and involved spinal canal (green) were confirmed manually by using Edit Mask (Draw and Erase) on the (A) coronal, (B) axial, and (D) sagittal views. (B,C) The cross-sectional contour of the spinal canal (red) with the widest distance between the pedicles at the same segment was defined as the boundary of the normal spinal canal in the region without pedicles. (E) 3D renderings of the OLF mass and spinal canal were reconstructed based on the outlines. The volume of the OLF mass (yellow) outside of the spinal canal (green) were then removed manually by using Edit Mask (Erase). (F) The ultimate 3D model was obtained, and the 3D OR (OLF volume/normal canal volume × 100%) was calculated automatically. 3D, 3-dimensional; OR, occupying ratio; OLF, ossification of the ligamentum flavum.

distance and no ossification between the pedicles at the same segment was defined as the boundary of the normal spinal canal (*Figure 4A-4D*). Therefore, the outline of the normal spinal canal was determined manually using Edit Mask. (III) The OLF mass was initially segmented by a threshold value of bone (226–1,751 HU). Based on the initial segmentation, the segment of maximum compression was chosen by Crop Mask. (IV) The outline of the OLF was further determined manually by using Edit Mask (*Figure 4A-4D*). Additionally, the outline of the OLF mass was limited to the outline of the normal spinal canal. (V) After 3D renderings were reconstructed based on the outlines, the Mask 3D Preview pattern was chosen, and the volume of the OLF mass outside of the spinal canal was further removed manually by using Edit Mask (Erase) (*Figure 4E*). Finally, the 3D models of the OLF and spinal canal were obtained (*Figure 4F*).

The 3D OR was calculated as follows: 3D OR = OLF volume/normal canal volume × 100%. The OLF volume was defined as the volume of ossified mass at the segment of maximum compression. The normal canal volume was defined as the volume of the spinal canal corresponding to the measured OLF (the top and bottom of the normal spinal canal were consistent with the top and bottom of the measured OLF).

Statistical analysis

MedCalc 19.0 (MedCalc Software Ltd, Inc., Ostend, Belgium) software was used for statistical analysis. Univariate analysis was performed to compare related variables between the DO and non-DO groups by independent *t*-test for continuous variables and chi-square tests for categorical variables. The reproducibility and reliability of the measurements were assessed by intraclass and interclass correlation coefficients, respectively. Receiver operating characteristic (ROC) curve analysis was performed to determine the optimal cutoff value of the 3D OR for distinguishing between patients with DO and those without DO. A comparison of the diagnostic value of the radiological parameters was performed based on the areas under the ROC curves (AUC) by *z* test. The level of statistical significance was set at a P value of 0.05

Results

After filtering, 283 patients were excluded and 114 patients were enrolled in this study (*Figure 1*). These patients were divided into the non-DO group (n=60) and the DO group (n=54). *Table 1* demonstrates that no significant differences in age (P=0.23), sex (P=0.54), BMI (P=0.39), DM (P=0.19),

Table 1 Univariate analysis of the related variables

Variable	Non-DO group	DO group	P value
No. of patients, n (%)	60 (52.6)	54 (47.4)	–
Age (years)	55.9±10.5	58.5±12.5	0.23
Sex, n (%)			0.54
Female	20 (33.3)	21 (38.9)	
Male	40 (66.7)	33 (61.1)	
BMI (kg/m^2)	25.6±3.5	26.3±4.3	0.39
DM, n (%)	6 (10.0)	10 (18.5)	0.19
HTN, n (%)	11 (18.3)	14 (25.9)	0.33
Number of involved segments	2.2±1.1	2.4±1.3	0.40
Segment of maximum compression, n (%)			0.61
Upper (T1–T4)	16 (26.7)	11 (20.4)	
Middle (T5–T8)	7 (11.7)	9 (16.7)	
Lower (T9–T12)	37 (61.6)	34 (62.9)	
3D OR (%)	30.8±7.5	50.9±7.9	<0.01*

The data are shown as n (%) or mean ± SD. *, statistically significant. DO, dural ossification; BMI, body mass index; DM, diabetes mellitus; HTN, hypertension; 3D, 3-dimensional; OR, occupying ratio.

Table 2 Cutoff values of the severity and range of OLF compression in the whole thoracic spine (T1–T12)

3D OR (%)	Sensitivity (%)	Specificity (%)	Diagnostic coincidence rate (%)
>37.0	100.0	81.7	90.4
>40.0	92.6	90.0	91.2
>43.0	79.6	98.3	89.5

OLF, ossification of the ligamentum flavum; 3D, 3-dimensional; OR, occupying ratio.

HTN (P=0.33), number of involved segments (P=0.40), or segments of maximum compression (P=0.61) distribution were found between the non-DO and DO groups. Most parts of the segments of maximum compression were located in the lower thoracic spine (T9–T12) (62.3%), while the remaining parts were in the upper and middle thoracic spine (T1–T8; 37.7%).

OLF compression and DO

The 3D OR in the DO group (50.9%±7.9%) was significantly higher than that in the non-DO group (30.8%±7.5%; P<0.01). The intraclass and interclass correlation coefficients were 0.94 and 0.90, respectively, demonstrating almost perfect agreement. *Table 2* shows that the 3D OR had a relatively high diagnostic accuracy for DO in the whole thoracic spine (T1–T12; 92.6% sensitivity, 90.0% specificity, and 91.2% diagnostic coincidence rate). The optimal cutoff point for the 3D OR was measured at 40.0% by the maximum of the Youden index.

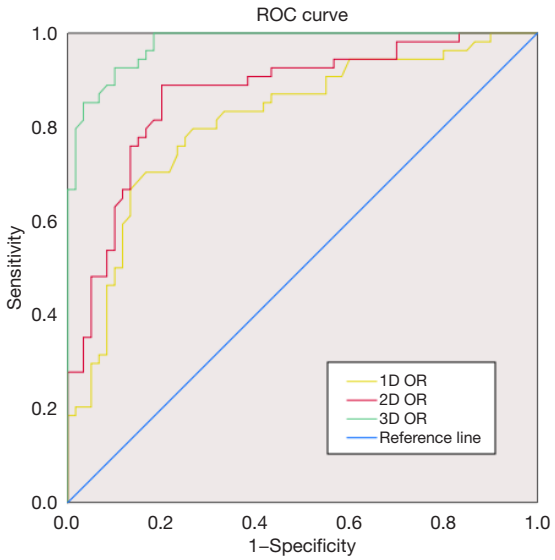

Figure 5 ROC curves of the 1D, 2D, and 3D ORs. ROC, receiver operating characteristic; 1D, 1-dimensional; 2D, 2-dimensional; 3D, 3-dimensional; OR, occupying ratio.

Comparison of the diagnostic value

The ROC curves of radiographic parameters in the whole thoracic spine (T1–T12) are illustrated in *Figure 5*. The 3D OR [AUC =0.98; 95% confidence interval (CI): 0.93–0.99] indicated a statistically higher diagnostic value for DO in the whole thoracic spine compared with the 1D OR (AUC =0.81; 95% CI: 0.73–0.88; P<0.01) and 2D OR (AUC =0.87; 95% CI: 0.79–0.92; P<0.01; *Table 3*). Additionally, the 2D OR had a higher diagnostic coincidence rate compared with the 1D OR despite the lack of statistical difference in their diagnostic values (P=0.18).

As shown in *Tables 4,5*, the 3D OR demonstrated a statistically higher and more stable diagnostic value than did the 1D OR and 2D OR regardless of whether it was applied in the upper and middle thoracic spine (T1–T8) or lower

Table 3 Comparison of the radiographic parameters in the whole thoracic spine (T1-T12)

Parameters	AUC	95% CI	Diagnostic coincidence rate (%)	P value
1D OR	0.81	0.73–0.88	77.2	–
2D OR	0.87	0.79–0.92	83.3	–
3D OR	0.98	0.93–0.99	91.2	–
3D OR *vs.* 1D OR	–	–	–	<0.01*
3D OR *vs.* 2D OR	–	–	–	<0.01*
1D OR *vs.* 2D OR	–	–	–	0.18

*, statistically significant. AUC, area under the curve; 1D, 1-dimensional; 2D, 2-dimensional; 3D, 3-dimensional; OR, occupying ratio.

Table 4 Comparison of the radiographic parameters in the upper and middle thoracic spine (T1–T8)

Parameters	AUC	95% CI	Diagnostic coincidence rate (%)	P value
1D OR	0.79	0.63–0.90	74.4	–
2D OR	0.83	0.68–0.93	79.1	–
3D OR	0.98	0.89–1.00	90.7	–
3D OR *vs.* 1D OR	–	–	–	<0.01*
3D OR *vs.* 2D OR	–	–	–	0.02*
1D OR *vs.* 2D OR	–	–	–	0.57

*, statistically significant. AUC, area under the curve; 1D, 1-dimensional; 2D, 2-dimensional; 3D, 3-dimensional; OR, occupying ratio.

Table 5 Comparison of the radiographic parameters in the lower thoracic spine (T9–T12)

Parameters	AUC	95% CI	Diagnostic coincidence rate (%)	P value
1D OR	0.84	0.73–0.91	81.7	–
2D OR	0.90	0.81–0.96	85.9	–
3D OR	0.97	0.90–0.99	91.6	–
3D OR *vs.* 1D OR	–	–	–	<0.01*
3D OR *vs.* 2D OR	–	–	–	0.04*
1D OR *vs.* 2D OR	–	–	–	0.16

*, statistically significant. AUC, area under the curve; 1D, 1-dimensional; 2D, 2-dimensional; 3D, 3-dimensional; OR, occupying ratio.

thoracic spine (T9–T12). Conversely, the diagnostic values of 1D OR and 2D OR in the upper and middle thoracic spine were markedly lower than those in the lower thoracic spine.

Clinical feasibility

As shown in *Table 2* and *Figure 6*, there was an obvious overlap between the DO and non-DO patients near the optimal cutoff value of 40% (from 37% to 43%). None of the DO patients had a 3D OR of <37% (100% sensitivity), while only 1 patient without DO had a 3D OR of >43% (98.3% specificity). This indicated that DO could be entirely excluded when the 3D OR was <37%, and could almost be diagnosed if the 3D OR was >43%. Therefore, the 3D OR was divided into 3 zones to maximize the clinical feasibility: the safe zone (<37%), vague zone (37–43%), and ossification zone (>43%).

Discussion

The major findings of this study were as follows. First, DO was significantly associated with the severity and range of OLF compression of the dura mater, and the 3D OR may be used as an indicator of DO in the whole thoracic spine. Second, the 3D OR demonstrated a statistically higher and more stable diagnostic value than did the 1D OR and 2D OR in the upper and middle thoracic spine (T1–T8), the lower thoracic spine (T9–T12), and the whole thoracic spine (T1–T12). Third, to maximize clinical feasibility, the 3D OR was divided into 3 zones: the safe zone (<37%), vague zone (37–43%), and ossification zone (>43%).

If the probability of DO could not be foreseen preoperatively, the risk of surgical complications, especially CSF leakage and spinal cord injury, would increase considerably (9). Although imaging signs such as the "comma sign" and "tram track sign" have been proposed for the diagnosis of DO, their misdiagnosis rates were reported to be 38.9%. Therefore, it might be necessary to develop a novel diagnostic method. In this study, we first proposed that the formation of DO was associated with the severity of OLF compression of the dura mater and the contact area of the OLF and the dura mater. However, it is difficult to simultaneously assess the severity and range of compression based only on the 1D or 2D radiological parameters (14,21). Our previous study found that the 3D OR could precisely reflect the oppressive state of OLF from multiple dimensions and thus predict the clinical grade of thoracic

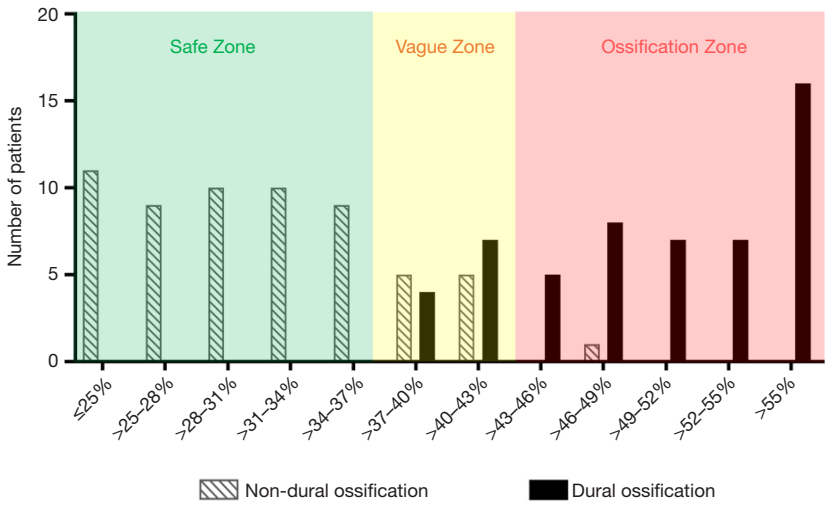

Figure 6 Distribution of the 3D OR in the whole thoracic spine for the diagnosis of DO in patients with OLF. 3D, 3-dimensional; OR, occupying ratio; DO, dural ossification; OLF, ossification of the ligamentum flavum.

myelopathy (14). Herein, we introduce the 3D OR to test this hypothesis and report whether it could be used as an indicator to identify DO in patients with OLF.

The univariate analysis indicated that the 3D OR in the DO group was significantly higher than that in the non-DO group, which suggested an association between the formation of DO and the severity and range of OLF compression. In the early stage of OLF, ossification usually grows from the capsular portion to the laminar portion (6). Furthermore, there is only mild spinal stenosis and no DO. With the progression of OLF, the ossification enlarges anteriorly toward the dura mater, thereby aggravating the severity of compression, resulting in deformation of the dura mater (23). At the same time, ossification also expands superiorly and inferiorly, thus enlarging the range of OLF compression of the dura mater (24). This increases the contact area of relative movement between the OLF and the dura mater (25). When the severity of OLF horizontal compression of the dura mater and their vertical contact area develops to a certain degree, DO might occur. Consistent with our hypothesis, the optimal cutoff point of the 3D OR was measured at 40.0%. ROC curve analysis indicated that the 3D OR had a high diagnostic value (92.6% sensitivity, 90.0% specificity, and 91.2% diagnostic coincidence rate) and could serve as a critical indicator for distinguishing between OLF patients with and without DO.

Considering that the formation of DO with OLF compression is a slowly progressive process, a single cutoff value might not correctly distinguish between DO and non-DO in OLF. In our study, there was an obvious overlap between patients with DO and those without DO near the 40% cutoff value (from 37–43%). However, none of the patients with DO had a 3D OR of <37%, while only 1 patient without DO had a 3D OR of >43%. For clinical feasibility, the 3D OR was divided into 3 zones: the safe zone (<37%), vague zone (37–43%), and ossification zone (>43%). For patients with OLF in the ossification zone, surgeons must realize the presence of DO and develop a normalized preoperative design that should contain a low-risk surgical procedure, proper management of the ossified thecal sac, and a rescue plan for CSF leakage after resection. For those in the vague zone, DO might be immature or may already exist. Thus, it is necessary to combine with other diagnostic methods, such as imaging signs, to further identify the presence of DO. For those in the safe zone, early surgical intervention is recommended to decrease the incidence of DO-related complications.

To our knowledge, this is the first study to compare the diagnostic value of radiographic parameters from 1D to 3D for DO. After analyzing 39 patients with OLF, Zhou *et al.* proposed that a unilateral spinal canal occupational rate (1D OR) could serve as an indicator of DO, reporting a 76.0% sensitivity and 91.0% specificity (12). In addition, Yu *et al.* reported a cross-sectional area OR (2D OR) that had 92.6% sensitivity and 96.6% specificity for the diagnosis of DO after analyzing 56 patients with OLF (15). However, comparing the sensitivity or specificity alone, rather than a statistical comparison, is insufficient to determine whether

these parameters are helpful in diagnosing DO (14,26). Furthermore, a small sample size could produce a type II error in the diagnostic model. Therefore, we analyzed 114 patients with OLF from 4 institutions and used the z test for comparison between independent ROC curves of these parameters (27). The 3D OR showed a statistically higher diagnostic value for DO in the whole thoracic spine compared with the 1D OR and 2D OR. A combination of factors might have contributed to this result and thus each part of the thoracic spine was investigated in detail.

DO in the upper and middle thoracic spine was previously reported to account for 33–46% of all DO cases. However, few studies have focused on the diagnostic efficacy of the conventional measurement methods for DO in T1–T8. Our results indicated that the diagnostic value of 1D OR and 2D OR in T1–T8 was markedly lower than that in T9–T12. Due to a large curvature variation between each segment in the upper and middle thoracic spine, it would be clinically wrong to perform these calculations without MPR. In contrast, this issue might be avoided by using the 3D imaging analysis. To correctly determine the radiological parameters, the 2D MPR can be reconstructed at an arbitrary angle or plane to achieve the appropriate orthogonal alignment based on a spinal section (14,28). This could explain why the 3D OR demonstrated a statistically higher and more stable diagnostic value for DO than did the 1D and 2D OR in T1–T8.

To eliminate the impact of MPR on the diagnostic value, these radiological parameters were further compared in the lower thoracic spine (T9–T12). Our results indicated that the 3D OR had a higher diagnostic value for DO in T9–T12 compared to that of the 1D and 2D parameters ($P<0.01$). Additionally, the 2D OR showed a higher diagnostic coincidence rate compared with the 1D OR, but this difference was not statistically significant. In fact, the 1D OR could only assess the degree of unilateral compression of OLF (9). Although the 2D OR could reflect the degree of bilateral compression, it could not assess the range of compression (14). Several radiographic parameters have been linked to OLF compression in previous studies, including the sagittal, coronal, and axial dimensions, which highlights the inadequacy of assessment from only a single dimension (9,12-14,29-31). In contrast, the 3D OR could make up for this owing to its comprehensive assessment of OLF compression from multiple dimensions.

This study has several limitations that should be noted. First, although our study included the largest sample size in the literature on the diagnosis of DO to date, its design was retrospective in nature. Therefore, a larger prospective study is needed to verify our findings. Second, our measurement method required manual operations in some key procedures, which might have inevitably produced human errors. However, the results still indicated that the 3D OR measurement method showed strong reproducibility and reliability. Third, the 3D imaging analysis based on Mimics software requires greater time and effort compared to the conventional measurement methods. Thus, further research is needed to simplify the operating steps and minimize human error in the future.

Conclusions

DO was significantly associated with the severity of OLF compression of the dura mater and the contact area of the OLF and the dura mater. The 3D OR could be used as a critical diagnostic indicator for identifying DO in the whole thoracic spine and showed superiority over the conventional radiological parameters. Classification of the 3D OR could maximize its clinical feasibility, thereby helping surgeons to decrease the incidence of DO-related surgical complications.

Acknowledgments

Funding: This study was supported by the National Natural Science Foundation of China (No. 81802218).

Footnote

Reporting Checklist: The authors have completed the STARD reporting checklist. Available at https://qims.amegroups.com/article/view/10.21037/qims-22-418/rc

Conflicts of Interest: All authors have completed the ICMJE uniform disclosure form (available at https://qims.amegroups.com/article/view/10.21037/qims-22-418/coif). The authors have no conflicts of interest to declare.

Ethical Statement: The authors are accountable for all aspects of the work in ensuring that questions related to the accuracy or integrity of any part of the work are appropriately investigated and resolved. This study was conducted in accordance with the Declaration of Helsinki (as revised in 2013) and was approved by and registered with the institutional review board of Shanghai Changzheng Hospital. The requirement for individual informed consent

for this retrospective analysis was waived.

References

1. Chen G, Fan T, Yang X, Sun C, Fan D, Chen Z. The prevalence and clinical characteristics of thoracic spinal stenosis: a systematic review. Eur Spine J 2020;29:2164-72.
2. Li X, An B, Gao H, Zhou C, Zhao X, Ma H, Wang B, Yang H, Zhou H, Guo X, Zhu H, Qian J. Surgical results and prognostic factors following percutaneous full endoscopic posterior decompression for thoracic myelopathy caused by ossification of the ligamentum flavum. Sci Rep 2020;10:1305.
3. Saiwai H, Okada S, Hayashida M, Harimaya K, Matsumoto Y, Kawaguchi KI, Kobayakawa K, Maeda T, Ohta H, Shirasawa K, Tsuchiya K, Terada K, Kaji K, Arizono T, Saito T, Fujiwara M, Iwamoto Y, Nakashima Y. Surgery-related predictable risk factors influencing postoperative clinical outcomes for thoracic myelopathy caused by ossification of the posterior longitudinal ligament: a multicenter retrospective study. J Neurosurg Spine 2019. [Epub ahead of print]. doi: 10.3171/2019.10.SPINE19831.
4. Daniels AH, McDonald CL, Basques BA, Kuris EO. Ossified Ligamentum Flavum: Epidemiology, Treatment, and Outcomes. J Am Acad Orthop Surg 2022;30:e842-51.
5. Chang SY, Kim Y, Kim J, Kim H, Kim HJ, Yeom JS, Lee CK, Chang BS. Sagittal Alignment in Patients with Thoracic Myelopathy Caused by the Ossification of the Ligamentum Flavum: A Retrospective Matched Case-Control Study. Spine (Phila Pa 1976) 2021;46:300-6.
6. Tang CYK, Cheung KMC, Samartzis D, Cheung JPY. The Natural History of Ossification of Yellow Ligament of the Thoracic Spine on MRI: A Population-Based Cohort Study. Global Spine J 2021;11:321-30.
7. Zhao Y, Xiang Q, Jiang S, Lin J, Wang L, Sun C, Li W. Incidence and risk factors of dural ossification in patients with thoracic ossification of the ligamentum flavum. J Neurosurg Spine 2022. [Epub ahead of print]. doi: 10.3171/2022.7.SPINE22645.
8. Li B, Qiu G, Guo S, Li W, Li Y, Peng H, Wang C, Zhao Y. Dural ossification associated with ossification of ligamentum flavum in the thoracic spine: a retrospective analysis. BMJ Open 2016;6:e013887.
9. Zhai J, Guo S, Zhao Y, Li C, Niu T. The role of cerebrospinal fluid cross-section area ratio in the prediction of dural ossification and clinical outcomes in patients with thoracic ossification of ligamentum flavum. BMC Musculoskelet Disord 2021;22:701.
10. Chen G, Chen Z, Li W, Jiang Y, Guo X, Zhang B, Tao L, Song C, Sun C. Banner cloud sign: a novel method for the diagnosis of dural ossification in patients with thoracic ossification of the ligamentum flavum. Eur Spine J 2022;31:1719-27.
11. Chen G, Zhang B, Tao L, Chen Z, Sun C. The diagnostic accuracy of CT-based "Banner cloud sign" for dural ossification in patients with thoracic ossification of the ligamentum flavum: a prospective, blinded, diagnostic accuracy study protocol. Ann Transl Med 2020;8:1606.
12. Zhou SY, Yuan B, Chen XS, Li XB, Zhu W, Jia LS. Imaging grading system for the diagnosis of dural ossification based on 102 segments of TOLF CT bone-window data. Sci Rep 2017;7:2983.
13. Lee BJ, Park JH, Jeon SR, Rhim SC, Roh SW. Clinically significant radiographic parameter for thoracic myelopathy caused by ossification of the ligamentum flavum. Eur Spine J 2019;28:1846-54.
14. Yan C, Tan HY, Ji CL, Yu XW, Jia HC, Li FD, Jiang GC, Li WS, Zhou FF, Ye Z, Sun JC, Shi JG. The clinical value of three-dimensional measurement in the diagnosis of thoracic myelopathy caused by ossification of the ligamentum flavum. Quant Imaging Med Surg 2021;11:2040-51.
15. Yu L, Li B, Yu Y, Li W, Qiu G, Zhao Y. The Relationship Between Dural Ossification and Spinal Stenosis in Thoracic Ossification of the Ligamentum Flavum. J Bone Joint Surg Am 2019;101:606-12.
16. Zhou SY, Yuan B, Qian C, Chen XS, Jia LS. Evaluation of Measuring Methods of Spinal Canal Occupation Rate in Thoracic Ossification of Ligamentum Flavum. World Neurosurg 2018;110:e1025-30.
17. Li B, Qiu G, Zhao Y. A potential method for identifying dural ossification by measuring the degree of spinal stenosis in thoracic ossification of ligamentum flavum. Med Hypotheses 2016;96:9-10.
18. Yamada T, Shindo S, Yoshii T, Ushio S, Kusano K, Miyake

N, Arai Y, Otani K, Okawa A, Nakai O. Surgical outcomes of the thoracic ossification of ligamentum flavum: a retrospective analysis of 61 cases. BMC Musculoskelet Disord 2021;22:7.
19. Endo T, Koike Y, Hisada Y, Fujita R, Suzuki R, Tanaka M, Tsujimoto T, Shimamura Y, Hasegawa Y, Kanayama M, Yamada K, Iwata A, Sudo H, Ishii M, Iwasaki N, Takahata M. Aggravation of Ossified Ligamentum Flavum Lesion Is Associated With the Degree of Obesity. Global Spine J 2021. [Epub ahead of print]. doi: 10.1177/21925682211031514.
20. Ju JH, Kim SJ, Kim KH, Ryu DS, Park JY, Chin DK, Kim KS, Cho YE, Kuh SU. Clinical relation among dural adhesion, dural ossification, and dural laceration in the removal of ossification of the ligamentum flavum. Spine J 2018;18:747-54.
21. Lee N, Ji GY, Shin HC, Ha Y, Jang JW, Shin DA. Usefulness of 3-dimensional Measurement of Ossification of the Posterior Longitudinal Ligament (OPLL) in Patients With OPLL-induced Myelopathy. Spine (Phila Pa 1976) 2015;40:1479-86.
22. An SB, Lee JJ, Kim TW, Lee N, Shin DA, Yi S, Kim KN, Yoon DH, Ha Y. Evaluating the differences between 1D, 2D, and 3D occupying ratios in reflecting the JOA score in cervical ossification of the posterior longitudinal ligament. Quant Imaging Med Surg 2019;9:952-9.
23. Sakai K, Yoshii T, Furuya T, Machino M. Research History, Pathology and Epidemiology of Ossification of the Posterior Longitudinal Ligament and Ligamentum Flavum. J Clin Med 2022;11:5386.
24. Du P, Ma L, Ding W. The influence of ossification morphology on surgery outcomes in patients with thoracic ossification of ligamentum flavum (TOLF). J Orthop Surg Res 2022;17:229.
25. Zhang H, Deng N, Zhang L, Zhang L, Wang C. Clinical Risk Factors for Thoracic Ossification of the Ligamentum Flavum: A Cross-Sectional Study Based on Spinal Thoracic Three-Dimensional Computerized Tomography. Risk Manag Healthc Policy 2022;15:1065-72.
26. Søreide K, Kørner H, Søreide JA. Diagnostic accuracy and receiver-operating characteristics curve analysis in surgical research and decision making. Ann Surg 2011;253:27-34.
27. Obuchowski NA, Bullen JA. Receiver operating characteristic (ROC) curves: review of methods with applications in diagnostic medicine. Phys Med Biol 2018;63:07TR01.
28. Shin DA, Ji GY, Oh CH, Kim KN, Yoon DH, Shin H. Inter- and Intra-Observer Variability of the Volume of Cervical Ossification of the Posterior Longitudinal Ligament Using Medical Image Processing Software. J Korean Neurosurg Soc 2017;60:441-7.
29. Feng F, Sun C, Chen Z. A diagnostic study of thoracic myelopathy due to ossification of ligamentum flavum. Eur Spine J 2015;24:947-54.
30. Lin J, Xu F, Jiang S, Wang L, Sun Z, Chen Z, Guo Z, Qi Q, Zeng Y, Sun C, Li W. Significance of body mass index on thoracic ossification of the ligamentum flavum in Chinese population. Eur Spine J 2022. [Epub ahead of print]. doi: 10.1007/s00586-022-07362-0.
31. Endo T, Takahata M, Koike Y, Fujita R, Suzuki R, Hisada Y, Hasegawa Y, Suzuki H, Yamada K, Iwata A, Sudo H, Yoneoka D, Iwasaki N. Association between obesity and ossification of spinal ligaments in 622 asymptomatic subjects: a cross-sectional study. J Bone Miner Metab 2022;40:337-47.

Cite this article as: Yan C, Ling SY, Zhao TY, Tan Y, Liu T, Shen J, Shi GD, Sun JC, Shi JG. Three-dimensional imaging analysis for the diagnosis of dural ossification in thoracic ossification of the ligamentum flavum: a multicenter study. Quant Imaging Med Surg 2023;13(1):417-427. doi: 10.21037/qims-22-418

